



Supplement of

GEMS ozone profile retrieval: impact and validation of version 3.0 improvements

Juseon Bak et al.

Correspondence to: Juseon Bak (juseonbak@pusan.ac.kr) and Jae-Hwan Kim (jaekim@pusan.ac.kr)

The copyright of individual parts of the supplement might differ from the article licence.

The copyright of individual parts of the supplement might differ from the article license.

To support the Airborne and Satellite Investigation of Asian Air Quality (ASIA-AQ) field campaign during February–March 2024, the GEMS operational observation schedule was revised following a coordination period from January 10 to January 31. After this adjustment period, the final revised schedule has been in operation since February 1, 2024.

(<https://nesc.nier.go.kr/en/html/board/bbs/24/select.do?pagingYn=Y&pageIndex=2&bbsManageInnb=24&bbsInnb=405>)

Table S1. GEMS Annual Observation Schedule (01 February 2024 – current)

No.	1	2	3	4	5	6	7	8	9	10	Total Observation Time
UTC	22:45	23:45	00:45	01:45	02:45	03:45	04:45	05:45	06:45	07:45	
KST	7:45	8:45	9:45	10:45	11:45	12:45	13:45	14:45	15:45	16:45	
Jan	X		FC	FC	FC	FC	FW	FW	FW	X	7
Feb	X	HE	FC	FC	FC	FC	FW	FW	FW	X	8
Mar	X	HE	FC	FC	FC	FC	FW	FW	FW	X	8
Apr	HE	HK	FC	FC	FC	FC	FW	FW	FW	FW	10
May	HE	HK	FC	FC	FC	FC	FW	FW	FW	FW	10
Jun	X	HK	FC	FC	FC	FC	FW	FW	FW	FW	9
Jul	X	HK	FC	FC	FC	FC	FW	FW	FW	FW	9
Aug	X	HK	FC	FC	FC	FC	FW	FW	FW	FW	9
Sep	X	HK	FC	FC	FC	FC	FW	FW	FW	FW	9
Oct	X	HE	FC	FC	FC	FC	FW	FW	FW	X	8
Nov	X	HE	FC	FC	FC	FC	FW	FW	FW	X	8
Dec	X		FC	FC	FC	FC	FW	FW	X	X	6

Table S2. GEMS Annual Observation Schedule (Initial – 01 January 2024)

No.	1	2	3	4	5	6	7	8	9	10	Total Observation Time
UTC	22:45	23:45	00:45	01:45	02:45	03:45	04:45	05:45	06:45	07:45	
KST	7:45	8:45	9:45	10:45	11:45	12:45	13:45	14:45	15:45	16:45	
Jan	X	X	HE	HK	FC	FW	FW	FW	X	X	6
Feb	X	X	HE	HK	FC	FW	FW	FW	X	X	7
Mar	X	HE	HK	FC	FC	FW	FW	FW	X	X	8
Apr	HE	HK	FC	FC	FC	FW	FW	FW	FW	FW	10
May	HE	HK	FC	FC	FW	FW	FW	FW	FW	FW	10
Jun	HE	HK	FC	FC	FW	FW	FW	FW	FW	FW	10
Jul	HE	HK	FC	FC	FW	FW	FW	FW	FW	FW	10
Aug	HE	HK	FC	FC	FW	FW	FW	FW	FW	FW	10
Sep	HE	HK	FC	FC	FW	FW	FW	FW	FW	FW	10
Oct	X	HE	HK	FC	FC	FW	FW	FW	FW	X	8
Nov	X	X	FC	HK	FC	FW	FW	FW	X	X	6
Dec	X	X	FC	HK	FC	FW	FW	FW	X	X	6

Table S3. List of fitting variables+, a priori values, and a priori errors. A correlation length of 6 km is used to construct the a priori covariance matrix for ozone variables, while all the other variables are assumed to be uncorrelated.

Fitting variables	# Variables	A priori	A priori error
Ozone at each layer	24	Climatology	Climatology
Surface albedo	1	Climatology	0.05
First-order wavelength-dependent term for surface albedo	1	0.0	0.01
Cloud fraction	1	Derived from 347 nm	0.05
Radiance/irradiance wavelength shifts	1	0.0	0.02 nm
Radiance/O ₃ cross section wavelength shifts	1	0.0	0.02 nm
Ring scaling parameters	1	-1.87	1
offset parameters in radiance	1	0.0	1.0 ⁻⁴
Slit width coefficient	1	0.0	0.1 nm
Shape factor coefficient	1	0.0	0.1

⁺The state vector elements are largely consistent with those used in Liu et al. (2010), except for the addition of the slit width and shape factor coefficients. The benefit of including these parameters was initially proposed by Bak et al. (2017), and was later adopted in the retrieval frameworks of Bak et al. (2024) and this study. The instrument slit function is assumed to follow a super-Gaussian shape, which is derived by fitting the irradiance spectrum and subsequently applied to radiance fitting. This approach compensates for differences between the slit functions of irradiance and radiance, and accounts for potential parameterization errors associated with the super-Gaussian approximation.

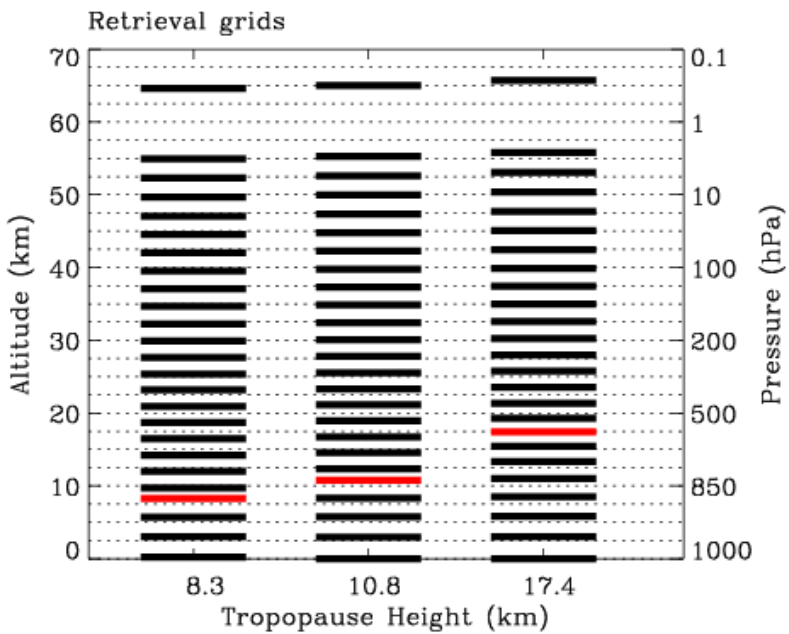


Figure S1. The 25 pressure levels used to retrieve partial ozone columns at 24 layers for three different atmospheric profiles, each with a distinct tropopause height (noted along the x-axis). The initial vertical pressure grid is defined as $P_i = 2^{-i/2}$ atm for $i = 0$ to 23, with the top-of-atmosphere pressure set at P_{24} . This grid is then adjusted by replacing the levels nearest to the surface pressure and thermal tropopause pressure. Tropospheric layers are redistributed evenly in logarithmic pressure space, with typically 3 to 7 layers assigned.

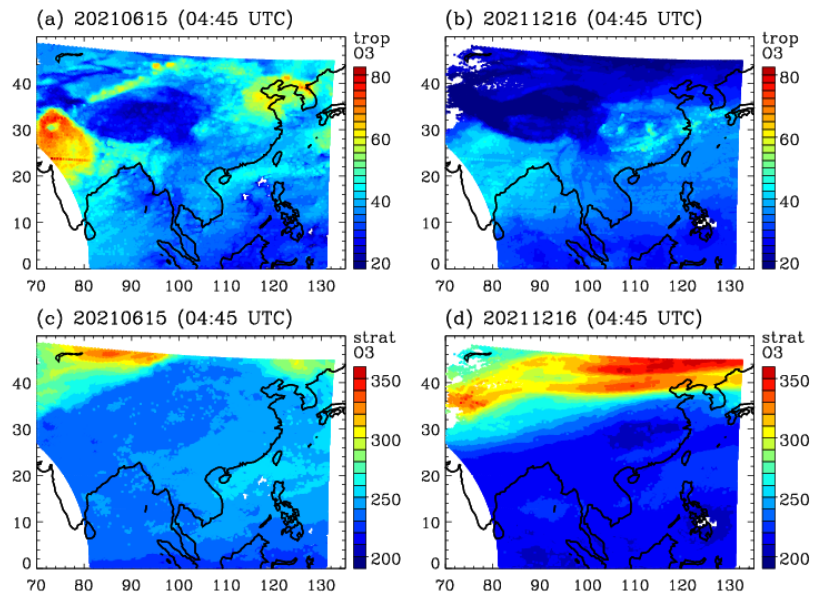


Figure S2. Tropospheric and stratospheric ozone column distributions on 15 June and 16 December 2021 (04:45 UTC).

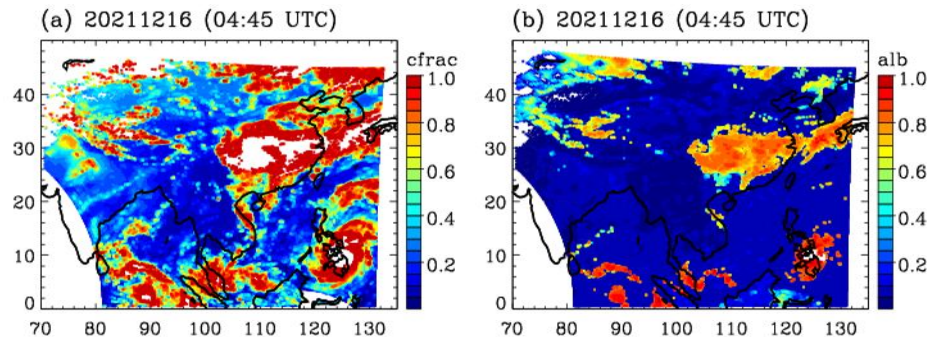


Figure S3. Same as Figure S2, but for the effective cloud fraction (input) and the fitted surface albedo (output) used in the ozone profile retrieval.

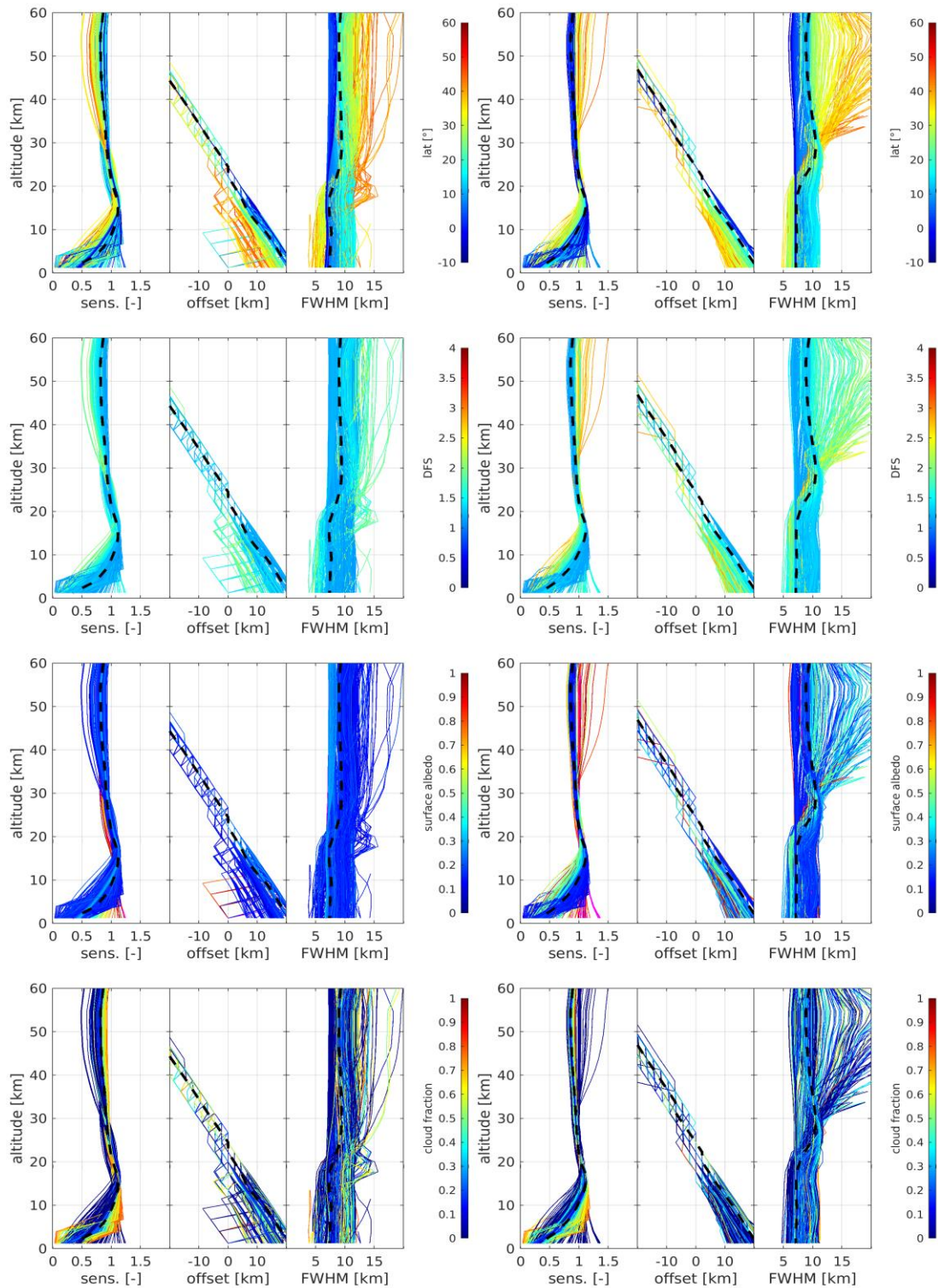


Figure S4. Information content of GEMS ozone profile retrievals in terms of sensitivity, offset, and kernel FWHM for 15 June (left) and 16 December (right), 2021. Each quantity is plotted as a function of four major influencing factors — from top to bottom panels: latitude, degrees of freedom for signal, surface albedo, and cloud fraction. Median values are indicated by black dashed lines.

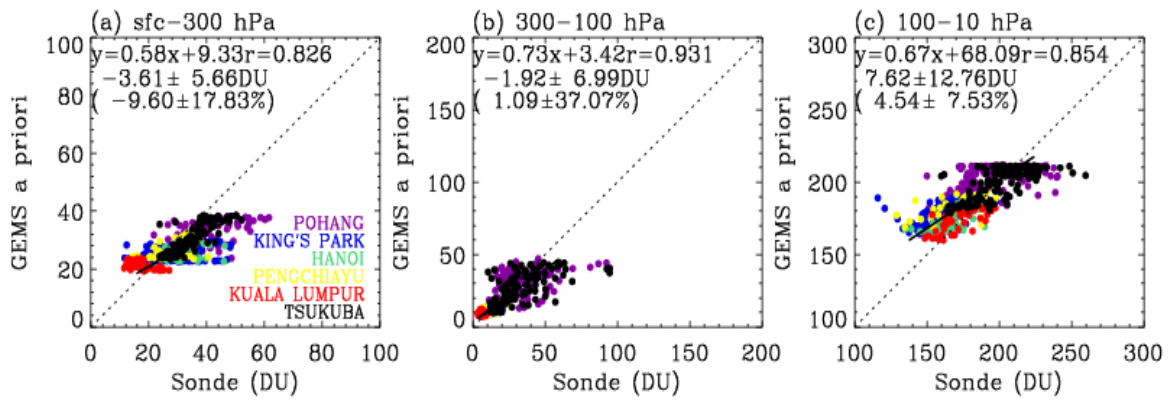


Figure S5. Same as Figure 11, but for scatters between GEMS a priori and ozonesonde measurements. The a priori is based on tropopause-based ozone profile climatology (Bak et al. 2013).